JOURNAL OF CATALYSIS **179,** 443–450 (1998)
ARTICLE NO. CA982238

The Evolution of Surface Species in NiW/Al_2O_3 Catalysts in Various Stages of Sulfidation: A Quasi *in-Situ* High Resolution Transmission Electron Microscopic Investigation

H. R. Reinhoudt,* A. D. van Langeveld,*,[1] P. J. Kooyman,† R. M. Stockmann,* R. Prins,‡ H. W. Zandbergen,† and J. A. Moulijn*

*Faculty of Applied Sciences, Delft University of Technology Julianalaan 136, 2628 BL Delft, The Netherlands; †National Center for High Resolution Electron Microscopy, Delft University of Technology, Rotterdamseweg 137, 2628 AL Delft, The Netherlands; ‡On leave from E.T.H. Zürich, Technisch/Chemisches Laboratorium, ETH Zentrum, CH 8092 Zürich, Switzerland

Received February 23, 1998; revised July 6, 1998; accepted July 9, 1998

The effect of the calcination temperature on the evolution of the active phase in NiW/γ-Al_2O_3 catalysts during sulfidation has been studied using high resolution transmission electron microscopy (HREM) and temperature programmed sulfidation (TPS). The evolution of the active phase is discussed in view of the performance of the catalysts in the hydrodesulfurization (HDS) of thiophene. Dependent on the pretreatment, three different species were observed with HREM: (i) subnanometer clusters (about 0.5 nm diameter), (ii) nanometer size particles (1 to 2 nm diameter), and (iii) WS_2-like slabs (2–3 nm length). The clusters and particles predominantly appear after low temperature sulfidation of catalysts calcined at 673 and 823 K. Hence, it is concluded that they are initially formed from the oxidic catalyst precursor. WS_2-like slabs are predominantly formed during high temperature sulfidation, independent of the calcination temperature. Activity measurements for the HDS of thiophene show that all phases exhibit a significant catalytic activity. HREM and activity measurements on various freshly sulfided and spent catalysts showed no significant differences in the catalysts prior to and after the reaction.

INTRODUCTION

In contrast to CoMo and NiMo catalysts, W-based catalysts such as NiW are employed much less frequently in the hydrotreating of oil. The reasons for it are that Ni-W based catalysts are more expensive than their CoMo-based counterparts and because they are less active in the bulk HDS of gasoil. As a consequence, W-based hydrotreating catalysts received much less attention in the literature than their Mo-based counterparts. However, for dedicated processes, where a high hydrogenation potential of the catalyst plays a key role, for instance in hydrodenitrogenation reactions or the deep HDS of diesel fuel, properly sulfided NiW-based catalysts could be an interesting option (1–9). Several studies on temperature-programmed sulfidation and reduction of NiW-based catalysts show that their susceptibility to sulfidation and reduction differs from those of NiMo and CoMo-based catalysts (10–13). The most important difference is that in case of NiW-based catalysts calcined at 673 K or higher temperature the sulfidation of the nickel oxide and the tungsten oxide occurs in two separate temperature regimes. In contrast to that, in conventionally prepared CoMo based catalysts both metal oxides sulfide almost simultaneously (14).

In the present investigation the effects of both the calcination and the sulfidation temperature on the genesis of the sulfidic phase are investigated with quasi *in-situ* high resolution transmission electron microscopy (HREM) and temperature programmed sulfidation (TPS). The results of these characterization methods are discussed in view of the performance of the various catalysts in the hydrodesulfurization (HDS) of thiophene.

EXPERIMENTAL

The catalysts were prepared by pore volume co-impregnation of crushed γ-Al_2O_3 (Ketjen 000-1.5E high purity, surface area 190 m^2/g, pore volume 0.60 ml/g, particle size 100–250 μm) with an aqueous solution of $(NH_4)_6W_{12}O_{39} \cdot xH_2O$ (Aldrich 35,897-5) and $Ni(NO_3)_2 \cdot 6H_2O$ (Aldrich 20,387-4). After impregnation, the precursor was dried at 393 K in static air for 16 h. Next, the dried catalyst was split into three equal portions, of which two were calcined in static air for 1 h at 673 or 823 K, the heating rate being 600 K h^{-1}. After calcination the three batches were analysed with AAS for their Ni and W content. For all three catalysts it was found to be 0.6 atom Ni/nm^2 (1.2 wt% Ni) and 2.7 atom W/nm^2 (15.6 wt% W), within limits of accuracy. The total metal loading corresponds to about 65% of the monolayer capacity of the support. In the text below, all catalysts will be referred to as "calcined."

[1] Corresponding author. E-mail: a.d.vanlangeveld@stm.tudelft.nl.

0021-9517/98 $25.00

Temperature-programmed sulfidation of the samples for HREM analysis was performed in a plug flow reactor at atmospheric pressure described in detail by Scheffer *et al.* (15, 16). About 100 mg of the crushed and sieved catalyst was diluted with an equal amount of SiC. After purging with Ar at room temperature, the catalyst was exposed to the sulfidation mixture containing H_2S, H_2, and Ar (3, 25, and 72 vol%, respectively) at a total flow rate of 33 μmol/s. After 0.5 h the temperature program was started at a linear heating rate of 600 K h^{-1}. Upon reaching the highest temperature of sulfidation, being 613 K, 673 K, 823 K, or 923 K, the sample was kept isothermal for 1 h, followed by a fast cooling to ambient temperature in the sulfidation mixture.

After purging with Ar, the reactor was closed, disconnected from the TPS equipment, and transferred into a glove box in which the partial pressure of O_2 and H_2O is typically less than 0.5×10^{-3} mbar in atmospheric Ar. Under these protective conditions, the catalyst was ground and suspended in *n*-hexane. A few droplets of the suspension were placed on a Cu grid coated with a Triafol microgrid sputtered with carbon (17). The grid was mounted in a high-vacuum compatible electron microscope holder, which can be closed for protective transport of the sample into the electron microscope. In the microscope, the holder was opened for HREM analysis of the sample. It should be stressed at this point that all samples have been transported into the electron microscope without exposure to air, that is, in the so-called "quasi *in-situ* mode." High resolution transmission electron microscopy was performed using a Philips CM30ST electron microscope equipped with a field emission gun operated at 300 keV and a Link EDX analyser. At least 15 representative areas of the catalyst surface were investigated and a minimum of 300 entities were counted to ascertain a statistically reliable evaluation.

The TPS signals in Fig. 1 were normalised to the amount of catalyst. The isothermal room temperature uptake, which always occurs directly after switching to the sulfidation mixture, is not shown in the spectra. However, it has been taken into account in the quantification of the degree of sulfidation, which for each catalyst at the various sulfidation temperatures mentioned above, was calculated from a TPS up to 923 K. The data were normalised to the sulfur uptake for a quantitative sulfidation of the nickel oxide and tungsten oxide into NiS and WS_2, respectively. Note that this degree of sulfidation may be somewhat lower than that of the actual catalyst analysed by HREM, since the latter has been exposed to a 1-h isothermal stage at the various temperatures.

Thiophene HDS was performed at 613 K in an atmospheric pressure plug-flow reactor. The particle size used was 170–500 μm. Sulfidation of the catalyst was done in H_2S/H_2 (15/85 vol%) at a total flow rate of 17 μmol/s. The catalyst was heated at 600 K h^{-1} to 543 K, kept isothermal for 0.5 h, followed by heating at a rate of 600 K h^{-1} to 613 K, 673 K, 823 K, or 923 K, respectively, where it was kept isothermal for 1 h. Because of the similarity of the sulfidation routines, it is expected that the catalysts investigated by HREM do represent those tested for their activity in the thiophene HDS. During thiophene HDS the total flow rate was 40 μmol/s, the thiophene content being 6 vol% in balance H_2. Thiophene conversions were determined after 4 h time on stream at 613 K in order to stabilise the catalysts.

RESULTS

Temperature-Programmed Sulfidation

The TPS profiles of all catalysts are presented in Fig. 1. For the performance testing the catalysts in the various stages of sulfidation and with a corresponding different speciation have been selected based on these TPS profiles. The

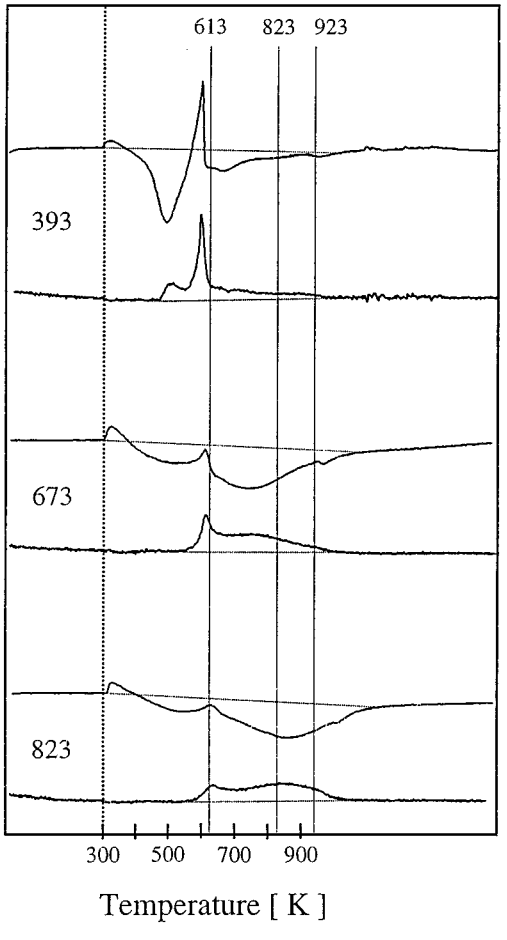

FIG. 1. TPS profiles of catalysts calcined at 393 K, 673 K, and 823 K, respectively. All signals are normalised to the amount of catalyst. A negative deflection of the H_2S profile (upper trace of each pair) corresponds to a H_2S consumption, whereas for H_2 (lower trace of each pair) a positive deflection corresponds to a H_2 consumption. The drying/calcination temperature (K) is indicated at the pairs of TPS profiles.

TABLE 1

The Degree of Sulfidation (in %) as Evaluated from Quantitative TPS

T_{sulf} (K) \ T_{calc} (K):	393	673	823
613	69	31	18
673	81	42	25
823	97	83	68
923	100	100	100

Note. Sulfidation to 100% is based on quantitative sulfidation into stoichiometric WS_2 and NiS.

selected temperatures of sulfidation and the corresponding degrees of sulfidation are summarised in Table 1.

For all catalysts, directly after the start of the heating programme a small amount of H_2S desorbs, since it is produced without accompanying H_2 consumption. In case of the catalyst calcined at 393 K, the H_2S consumption starts at about 380 K and accelerates from 410 K. Simultaneously with the latter, a small amount of H_2 is consumed. Both the H_2 and the H_2S profiles show a maximum consumption at about 490 K. At higher temperatures, a steeply increasing H_2S concentration can be seen. The latter effectively results in a H_2S production, with a peak at about 600 K. Simultaneously, a spike in the H_2 consumption can be observed. At still higher temperatures a smooth H_2S consumption occurs over a wide range of temperatures, simultaneously with a corresponding H_2 consumption. As can be seen in Table 1, the degree of sulfidation gradually increases from 69% at 613 K up to 100% at 923 K.

For the catalyst calcined at 673 K, the H_2S uptake starts at about 390 K, leading to a maximum uptake, i.e. a minimum in the H_2S concentration, at about 500 K. At higher temperatures, the H_2S concentration increases which results in a maximum H_2S concentration at about 600 K. Simultaneously, a maximum in the H_2 consumption occurs. The maximum in the H_2S concentration is followed by a second H_2S uptake with a maximum rate of consumption at about 700 K, followed by a slow progressive sulfidation of the sample up to 923 K. The sulfidation increases from about 31% at 613 K up to 100% at 923 K.

The TPS profile of the catalyst calcined at 823 K is very similar to that of the catalyst calcined at 673 K, only the following minor differences can be seen. The maximum rate of the H_2S production with simultaneous H_2 consumption has shifted to above 600 K, while the maximum rate of sulfidation in the second stage of sulfidation has shifted to about 770 K. Finally, the degree of sulfidation is lower, viz. 18% at 613 K and 100% at 923 K.

Electron Microscopy

Dependent on the pretreatment, three different features have been observed in the various catalysts:

(i) subnanometer clusters (about 0.5 nm diameter),
(ii) nanometer size particles (1 to 2 nm diameter), and
(iii) WS_2-like slabs with a length of about 2–3 nm.

When a freshly sulfided catalyst was exposed to air prior to HREM analysis, the slabs were more susceptible to electron beam induced damage than those of a sample introduced in the microscope under protective conditions (quasi *in situ*). Analogously, when a freshly sulfided catalyst was exposed to air after a quasi *in situ* electron microscopic analysis and reintroduced in the electron microscope, the slabs were also more susceptible to electron beam induced damage. In the electron beam induced decomposition, the slabs transferred into (spherical) particles, which are very similar to the nanometer size particles mentioned above under (ii). As a result, catalysts not introduced under protective conditions contain fewer slabs and more nanometer-sized particles than those introduced quasi *in situ*. Subnanometer clusters were not observed in catalyst samples exposed to air. Analogous results have been reported previously for molybdenum-based catalysts (18). Also, highly dispersed nickel sulfide catalysts, which were exposed to air briefly, clearly showed a significant degree of oxidation, as could be inferred from their X-ray photoelectron spectra (19, 20). Thus, all catalysts in this study have been introduced in the HREM in the quasi *in situ* mode, since this is essential for the occurrence of the various surface species. In addition to the freshly sulfided catalysts, also spent catalysts were investigated by HREM. From the comparison of the fresh and the spent catalysts and their activity patterns, it was concluded that various species observed are stable under the reaction conditions as applied in the current experiments.

The subnanometer clusters (Fig. 2a) have a size of about 0.5 nm, are visible due to a higher contrast as compared to their surroundings and are stable under the electron beam as applied. The nanometer size particles (Fig. 2b) have a spherical shape with a diameter between 1 and 2 nm. At low irradiation levels of the electron beam the particles are stable, however, no interference pattern due to the lattice planes could be observed because of the low intensity of the electron beam. At a higher intensity of the electron beam only for limited periods the images of the particles showed clear interference patterns; a major part of the time no interference patterns due to lattice planes could be observed. Each time that the interference pattern reappeared, the position of the lines was different, indicating a different orientation of the lattice planes in the particle with respect to the electron beam.

A typical example of WS_2-like slabs can be seen in Fig. 2c. The slabs are very similar to those reported in previous HREM studies on hydrotreating catalysts (21) and contain relative low concentrations Ni, as inferred from EDX analysis. In general, the slab-size increased to about 3 nm after sulfidation at 673 K and higher temperatures while a low

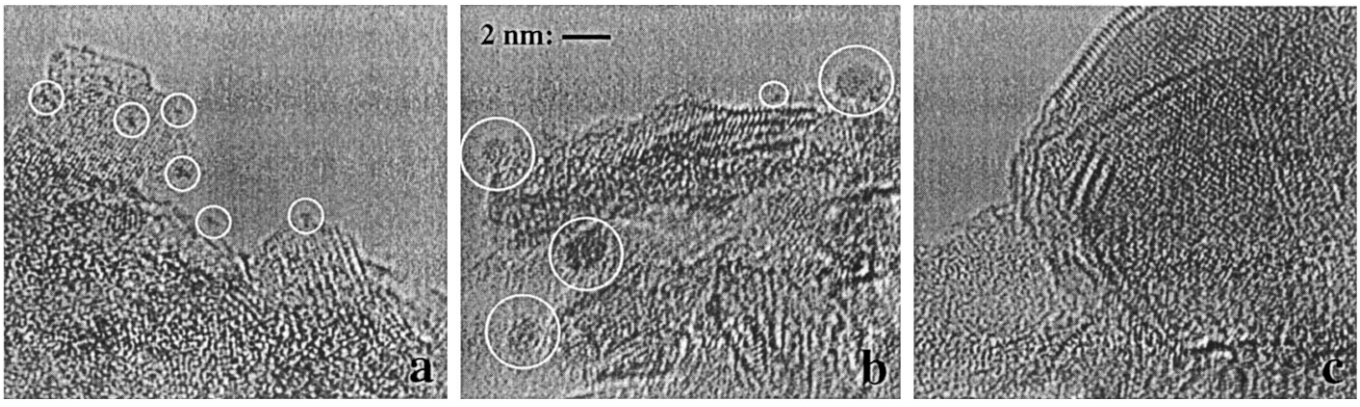

FIG. 2. Typical HRTEM images of (i) subnanometer clusters (Fig. 2a, catalyst calcined at 823 K and sulfided at 613 K), (ii) nanometer particles (Fig. 2b, catalyst calcined at 823 K and sulfided at 673 K), and (iii) slabs (Fig. 2c, catalyst calcined at 673 K and sulfided at 823 K). The magnification in the three images is equal, for ease of the interpretation a bar with a length of 2 nm is shown.

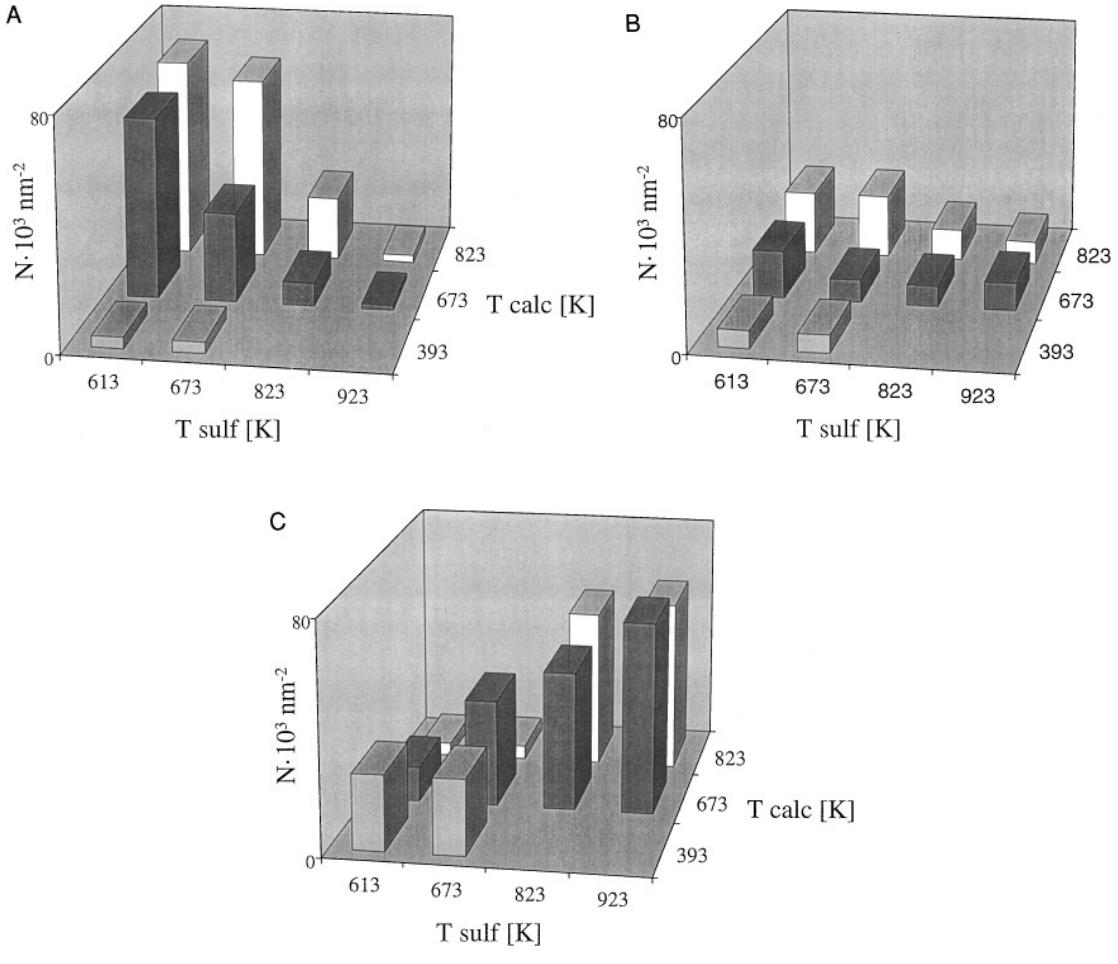

FIG. 3. Bar graphs as derived from the HREM micrographs of the various catalysts as a function of their calcination and sulfidation temperature in K. The density of the species, N, is normalised to the surface area of the catalysts and indicates the trend of the occurrence of the various species. The estimated accuracy in the data is about 10%, relatively. A, subnanometer clusters; B, nanometer particles; C, slabs.

average stacking degree of the slabs was observed under all circumstances.

Statistics of Electron Microscopy

A statistical analysis has been made on the occurrence of the subnanometer clusters, the nanometer size particles and the slabs in the various catalysts. Note that the densities have been defined as the number of species observed per 1000 nm^2 surface area of the alumina. The results are summarised in Figs. 3a–c as bar graphs, where the relative occurrence of the three species can be compared directly. It should be noted, however, that the bar graphs are meant to indicate a trend rather than to represent exact numbers.

For the subnanometer clusters a high density is found after sulfidation at 613 K of the catalysts calcined at 673 K and 823 K. The highest density of the nanometer-size particles is found after sulfidation at 673 K of the catalysts calcined at 823 K. For the 673 K calcined catalyst, the highest density of nanometer particles is found after sulfidation at 613 K. With increasing sulfidation temperatures the density of both the subnanometer clusters and the nanometer size particles decreases relatively fast for the 673 K calcined catalyst, as compared to the catalyst calcined at 823 K. In parallel, the slab density increases relatively fast in the 673 K calcined catalyst, as compared to that in the 823 K calcined catalyst.

For the catalyst calcined at 393 K followed by sulfidation at 613 K and 673 K, only limited numbers of nanometer particles and relatively large numbers of slabs are observed, in contrast to the catalysts calcined at higher temperatures.

Catalyst Activity in the HDS of Thiophene

Figure 4 gives the first-order reaction rate constant for the HDS of thiophene over the various catalysts as a function of their sulfidation temperature. Two different trends can be clearly observed. First, for a given calcination temperature, a progressively increasing activity can be observed with increasing sulfidation temperature up to 823 K; at still higher sulfidation temperatures the activity of the catalysts decreases for all catalysts. Second, the milder the calcination of a catalyst prior to its sulfidation, the better the performance of the catalyst in the HDS of thiophene. Within limits of experimental accuracy this difference levels off, however, when the catalyst is sulfided at or above its calcination temperature. When comparing the catalysts sulfided at 673 K and 823 K, one observes that for all catalysts a major change in the selectivity occurs after sulfidation at 823 K and higher temperatures, as can be seen in Fig. 5. At lower temperatures of sulfidation, all catalysts exhibit a relatively high selectivity for hydrogenation, whereas after sulfidation at 823 K and higher, the selectivity clearly shifts towards hydrogenolysis.

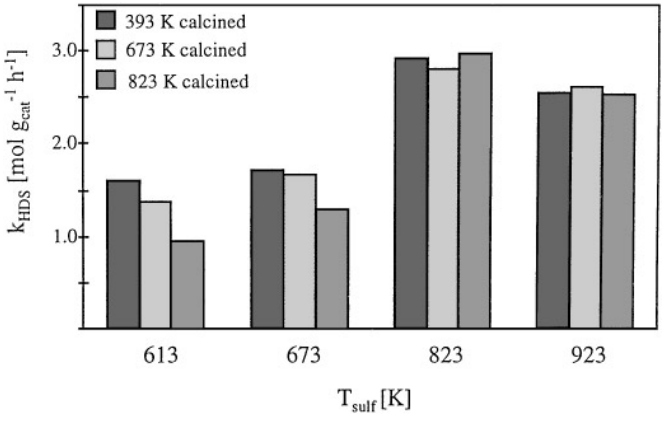

FIG. 4. The first-order overall reaction rate constants for thiophene HDS of the various catalysts calcined at 393 K, 673 K, and 823 K, followed by sulfidation at 613 K, 673 K, 823 K, and 923 K (reaction temperature 623 K, pressure 0.1 MPa, in a flow reactor).

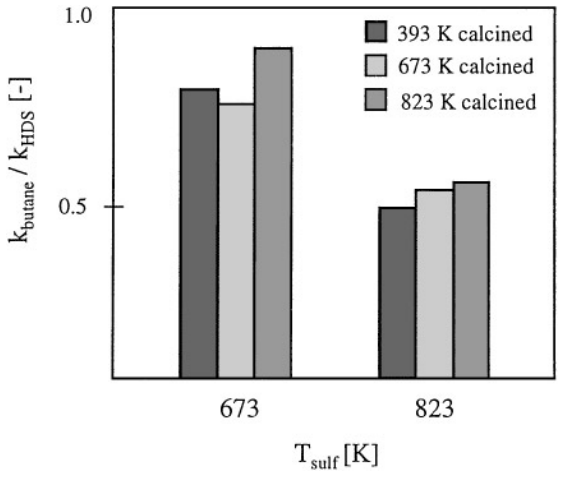

FIG. 5. The ratio of the first-order overall reaction rate constants of hydrogenation and thiophene HDS. The NiW catalysts were calcined at 393, 673, and 823 K, respectively, followed by sulfidation at 673 K and 823 K, respectively (reaction temperature 623 K, pressure 0.1 MPa, in a flow reactor).

For comparison a Ni/γ-Al_2O_3 and a W/γ-Al_2O_3 catalyst, calcined at 773 K and sulfided at 613 K, were tested in the thiophene HDS reaction. Their activities were at least one order of magnitude lower than that of their Ni-W based counterpart.

DISCUSSION

Dependent on the calcination temperature, in the oxidic Ni-W based catalysts the following species may occur: "micro-crystalline," highly dispersed nickel oxide, tungsten oxide, nickel-tungstate, and nickel-aluminate. After low temperature calcination, relative large amounts of nickel oxide and tungsten oxide are being formed, while after calcination at 673 K and higher temperatures the nickel oxide dissolves in the tungstate phase to form nickel tungstate, or reacts with the alumina to nickel-aluminate (1, 10, 22).

In the temperature-programmed sulfidation of the catalysts, three different regimes can be discerned. In the first regime up to about 600 K the "micro-crystalline" nickel oxide is sulfided in the calcined catalysts (1, 10). In contrast, for the catalyst calcined at 393 K, also a major part of the W must have exchanged its oxygen for sulfur in this first H_2S uptake, because of the high degree of sulfidation at 613 K (69%). Because of the large H_2 consumption peaking at about 590 K at least part of the sulfided tungsten is reduced from W^{6+} into W^{4+}. This is corroborated by the observation in HREM that a rather large number of slabs is formed already after sulfidation at 613 K (cf. Fig. 3c) of the 393 K calcined catalyst. This is also in line with the relatively high activity of this catalyst in the HDS of thiophene, as compared to that of the calcined catalysts (see Fig. 4). The nature of the small H_2 consumption, which peaks at about 500 K simultaneously with the sulfur uptake is not fully clear. It may be attributed to the reduction of tungsten, or to the decomposition of nitrates still present from the metal precursors. Whatever the case may be, in the 393 K calcined catalyst the tungstate is hardly stabilised by the alumina because of the weak interaction between both.

In the second regime at about 590 K, a sharp H_2S production and H_2 consumption are observed for the 393 K calcined catalyst. The shape of the peaks suggests that the process is kinetically limited rather than determined by thermodynamics. It could, for instance, be caused by the nickel catalysed reduction of a tungsten oxy-sulfide, or the hydrogenation of so-called "excess sulfur" (10, 23). A detailed quantitative analysis of the TPS profiles (22) clearly shows that this H_2S production can be correlated to the reduction of WS_3. The much smaller H_2 consumption and the correspondingly smaller maximum in the H_2S at about 600 K for the catalysts calcined at 673 and 823 K indicate the more refractory nature of the tungstate layer after calcination at 673 K and higher temperatures. This is also supported by the limited degree of sulfidation of the calcined catalysts at 613 K shown in Table 1.

In the third regime, starting at about 600 K, dependent on the calcination temperature, nickel tungstate and tungsten oxide are progressively sulfided while simultaneously W^{6+} is reduced into W^{4+}, as can be inferred from the H_2 consumption. This is in accord with the temperature programmed sulfidation of Ni-W based catalysts reported by Scheffer *et al.* (1). The high temperature shift of the maximum rate of H_2S uptake for the calcined catalysts again supports the more refractory nature of the tungstate after calcination at 673 K and 823 K.

Following calcination at 823 K, the degree of sulfidation of the active phase is strongly reduced (only 18% at 613 K sulfidation temperature) as compared to that of the 393 K calcined catalyst (69% at 613 K sulfidation temperature). This is also reflected in the XPS spectra of the Ni 2p emission line. After sulfidation at 613 K about 60% of the Ni is sulfided following calcination at 673 K, while after calcination at 823 K only 40% of the Ni is sulfided at 613 K (24).

High-resolution electron microscopy of the 673 K calcined catalysts sulfided at 613 K and the 823 K calcined catalysts sulfided at 613 K and at 673 K shows the presence of species with dimensions in the range of about 0.5 nm (Fig. 2a) which protrude from the catalyst surface. Since these clusters are not observed in the freshly calcined sample, they must have been formed during the sulfidation step. They are exclusively observed in the Ni-W-based catalyst after sulfidation and neither in sulfided W/γ-Al_2O_3 nor in sulfided Ni/γ-Al_2O_3. Finally, they are predominantly observed in the calcined catalysts sulfided at temperatures, where the highly dispersed nickel oxide is already sulfided and Ni in $NiWO_4$ (1, 10) just starts to sulfide. Since the Ni-W-based catalysts containing the subnanometer clusters exhibit a relatively high activity in the thiophene HDS (Fig. 4), in contrast to their Ni- and W-based counterparts, the activity of the Ni-W-based catalyst must be due to the combined action of Ni and W in close contact. Especially in view of their limited degree of sulfidation (only 18 to 31%), the catalytic activity of these catalysts in the HDS of thiophene is remarkably high. This observation is however, in line with recent work of Eijsbouts *et al.* (25) on fully sulfided high-activity CoMo-based catalysts. They investigated a series of similar catalysts with varying dispersion with electron microscopy and EXAFS analysis. From the combined results it was concluded that a substantial amount of the active phase was present as a highly dispersed species, not necessarily being slabs, containing at most seven Mo atoms. Clearly, such small species were not observed in their electron microscope. However, their electron microscopic analysis was performed under exposure of the catalysts to air (*ex situ*) in using quite different sample preparation and it was experienced in the current research that such small identities may disappear upon exposure of a catalyst to air. Whatever the case is, these observations clearly illustrate that also other species than the well-known slab-like "CoMoS" phase as proposed by Topsøe *et al.* (7) can play an active role in the hydrodesulfurization reaction.

At slightly higher sulfidation temperatures, nanometer size particles are observed simultaneously with the subnanometer clusters. The particles have a tendency to change shape and orientation at higher electron beam intensities, as for instance observed for small metallic particles (26). Since these nanometer sized particles are found predominantly in catalysts where W is in its initial stages of sulfidation, it is concluded that this species most likely represents an intermediate species in the process of sulfidation.

The appearance of slab-like structures in the sulfided, calcined catalysts occurs simultaneously with the disappearance of the sub-nanometer clusters, as can be seen in Figs. 3a and 3c. Especially at sulfidation temperatures of 823 K

and higher, predominantly WS_2-like slabs are observed, in which relatively low concentrations of Ni were found by EDX. That the occurrence of slabs coincides with the disappearance of the clusters and particles also indicates the transient nature of the latter two species. However, at present it is not clear if the subnanometer clusters are a nucleus for the formation of slabs, or if they are a separate phase which becomes thermodynamically unstable at higher sulfidation temperatures and transforms into the thermodynamically stable WS_2-like structures.

As for the role of the calcination step, at 823 K and higher calcination temperatures the bonding of the (nickel) tungstate layer to the alumina (1, 22) is established, while also more of the nickel tungstate is formed (1, 22, 27). This is corroborated by the present TPS and HREM observations, collected in Figs. 1 and 3. In the TPS profile (Fig. 1) of the 393 K calcined catalyst a relatively large H_2 consumption, simultaneously with a large H_2S uptake, which must also be attributed to the sulfidation of tungsten, is observed at temperatures below 600 K, in contrast to the catalysts calcined at 673 and 823 K. For the 393 K calcined catalyst significant amounts of slabs are observed after sulfidation at temperatures as low as 613 K. Also, the small number of subnanometer clusters in the 613 K sulfided, 393 K calcined catalyst as compared to its calcined counterparts is striking. After calcination at higher temperatures more nickel is stabilised by incorporation in $NiWO_4$, which is stabilised further by the alumina. Therefore, it can be concluded that the more refractory the nickel oxide and the tungsten oxide are before sulfidation, the more subnanometer clusters are being formed in the initial stages of sulfidation.

To summarise, the present observations indicate that the genesis of the surface species in a NiW/γ-Al_2O_3 catalysts upon sulfidation starts with the formation of subnanometer nickel sulfide clusters, likely containing some W. Under more severe sulfidation conditions also nanometer sized particles are formed. Both the clusters and the particles are most likely transformed into the well-known WS_2-like slabs, since the numbers of the former decrease in the HREM images with increasing sulfidation temperature, that is with increasing number of WS_2-like slabs. All catalysts containing the various species observed have a comparable activity in the HDS of thiophene.

The highest activity for HDS of thiophene is found for the catalysts sulfided at 823 K. TPS shows that in these catalysts part of the tungsten is reduced and sulfided into WS_2. HREM shows the presence of large numbers of WS_2-like slabs and only very low numbers of subnanometer clusters and limited numbers of nanometer sized particles. This suggests that the WS_2 based slab-like structures have a high activity in the HDS of thiophene, in accord with the so-called Topsøe model (7). However, in view of their limited degree of sulfidation and the absence of large numbers of slabs, the catalyst prepared by calcination at 823 K followed by sulfidation at 613 K has a remarkably high activity for the HDS of thiophene.

As for the role of the calcination temperature on the activity of the catalysts in the thiophene HDS, it can be seen in Fig. 4 that the lower the temperature of thermal treatment of the catalysts is, the higher their activity is at lower sulfidation temperatures. This difference disappears, however, after sulfidation at a temperature equal to, or higher than the calcination temperature. For instance, the difference between the 393 K and the 673 K calcined catalyst disappears after sulfidation at 673 K and higher temperatures. As a result, after sulfidation at 823 K all catalysts have about the same activity. The degree of sulfidation at 823 K as calculated from the TPS profiles of the various catalysts (see Table 1) is most likely lower than the actual degree of sulfidation of the catalysts tested for HDS and investigated by HREM, since the latter were sulfided isothermally during 1 h. In view of the TPS profiles it can be expected that all catalysts are quantitatively sulfided after 1 h at 823 K. In contrast, the differences in the degree of sulfidation at 613 K and 673 K (see Table 1) reflect actual differences of the actual catalysts. Hence, it is concluded that the different species play a role as active sites in HDS reactions. This is also supported by their activity in the HDS of thiophene shown in Fig. 4. The results clearly show that the 673 and 823 K calcined catalysts, which contain preferentially subnanometer clusters and almost no slab-like structures after low temperature sulfidation, have a relatively high activity as compared to the low temperature sulfided, 393 K calcined catalysts which preferentially contain slabs.

As can be seen in Figs. 3a and 3c, the morphology of the 823 K calcined catalyst essentially changes from subnanometer clusters in the 673 K sulfided catalyst into slab-like structures after sulfidation at 823 K. In Fig. 4, this transformation is reflected in strongly increased activity. Simultaneously with this, the selectivity for hydrogenation of butene to butane strongly decreases, supporting the transformation of the morphology of the catalytic active phase. Quite remarkably, however, the activities of the 393 K and the 673 K calcined catalysts also increase strongly in this temperature regime of sulfidation, while for both already a significant amount of the slab-like structures is observed in the catalyst sulfided at 673 K. Even more surprising is the strongly decreased selectivity for hydrogenation after sulfidation at 823 K, analogously to that of the 823 K calcined catalyst. Apparently, in view of their catalytic selectivity and activity, all catalysts sulfided at 673 K seem to consist of the same type of active species. After sulfidation at 823 K, the activity of all catalysts strongly increases and a distinct change in selectivity is observed. For the 823 K calcined catalyst this coincides with a strong increase in the slab density. One could conclude that the slabs observed in HREM are directly responsible for the observed changes in catalytic performance. However, for the 673 K calcined

catalyst, already after sulfidation at 673 K a high density of slabs is observed, without any indication for a difference in activity or selectivity, as compared to its 823 K calcined counterpart. Hence, the slab-like species observed in HREM of both catalyst samples do not necessarily represent the same active sites. In the sulfidation interval between 673 K and 823 K the slab-like phase apparently undergoes changes which are not easily observed with HREM but have a strong impact on the activity and selectivity of the catalyst. Therefore, observations made by HREM should be carefully interpreted in detail, since some trends in the catalytic performance may be correlated with observed changes in the electron microscope, whereas others are not reflected in changes in the electron microscope.

CONCLUSIONS

In the initial stages of sulfidation of an oxidic NiW/γ-Al_2O_3 catalyst, subnanometer clusters with a diameter of about 0.5 nm are formed. Most likely, this species contains both Ni and W since it is concluded that this species is unique for the bimetallic system. Under more severe sulfidation conditions WS_2-like slabs, containing Ni, are formed. At intermediate stages of sulfidation particles with a diameter of 1–2 nm are observed. All catalysts containing the various observed species exhibit a significant catalytic activity for the HDS of thiophene. A major difference in the activity and selectivity is observed for catalysts sulfided at 673 K and 823 K.

ACKNOWLEDGMENTS

These investigations were supported by the Netherlands Foundation for Chemical Research (SON) with financial aid from the Netherlands Technology Foundations (STW). E. Crezee is acknowledged for performing the thiophene activity measurements. Stimulating discussions with Dr. V. H. J. de Beer (Eindhoven University of Technology) are gratefully acknowledged. The research has been performed under the auspices of NIOK, the Netherlands Institute for Catalysis Research, Lab Report **TUD 98-4-883**.

REFERENCES

1. Scheffer, B., Mangnus, P. J., and Moulijn, J. A., *J. Catal.* **121**, 18 (1990).
2. LePage, J. F., *in* "Applied Heterogeneous Catalysis," Institut Francais des Petrol Publications, Paris, 1988.
3. Ahuja, S. P., Derrien, M. L., and LePage, J. P., *Indus. Eng. Chem. Prod. Res. Develop.* **9**, 272 (1970).
4. Vrinat, M., Lacroix, M., Breysse, M., and Frety, R., *Bull. Soc. Chim. Belg.* **93**, 697 (1984).
5. Cachet, C., Breysse, M., Cattenot, M., Dechamp, T., Frety, R., Lacroix, M., de Mourgues, L., Portefaix, J. L., Vrinat, M., Duchet, J. C., Housny, S., Lakhdar, M., Tilliette, M. J., Bachelier, J., Cornet, D., Engelhardt, P., Guegen, C., and Toulhoat, H., *Catal. Today* **4**, 7 (1988).
6. Grange, P., *Catal. Rev. Sci. Eng.* **21**, 135 (1980).
7. Topsøe, H., Clausen, B. S., and Massoth, F. E., *in* "Catalysis, Science and Technology" (J. R. Andersson and M. Boudart, Eds.), Vol. 11, Springer-Verlag, Berlin, 1996.
8. Kim, C-H., Yoon, W. L., Lee, I. C., and Woo, S. I., *Appl. Catal. A: General* **144**, 159 (1996).
9. Reinhoudt, H. R., Troost, R., Van Schalkwijk, S., Van Langeveld, A. D., Sie, S. T., Van Veen, J. A. R., and Moulijn, J. A., *Fuel Proc. Technol.*, submitted.
10. Mangnus, P. J., Bos, A., and Moulijn, J. A., *J. Catal.* **146**, 437 (1994).
11. Scheffer, B., Molhoek, P., and Moulijn, J. A., *Appl. Catal.* **46**, 11 (1989).
12. Mangnus, P. J., Scheffer, B., and Moulijn, J. A., *Prep. Am. Chem. Soc., Div. Petr. Chem.* **32**, 329 (1987).
13. Arnoldy, P., Franken, M. C., Scheffer, B., and Moulijn, J. A., *J. Catal.* **96**, 381 (1985).
14. Mangnus, P. J., Poels, E. K., and Moulijn, J. A., *I & EC Res.* **32**, 1818 (1993).
15. Scheffer, B., Van Oers, E. M., Arnoldy, P., De Beer, V. H. J., and Moulijn, J. A., *Appl. Catal.* **25**, 303 (1986).
16. Scheffer, B., Dekker, N. J. J., Mangnus, P. J., and Moulijn, J. A., *J. Catal.* **121**, 31 (1990).
17. Zandbergen, H.W., Pruymenboom, A., and Van Tendeloo, G., *Ultramicroscopy* **24**, 45 (1988).
18. Stockmann, R. M., Zandbergen, H. W., Van Langeveld, A. D., and Moulijn, J. A., *J. Molec. Catal. A: Chemical* **102**, 147 (1995).
19. Janssens, J.-P., Van Langeveld, A. D., Bonné, R. L. C., Lok, C. M., and Moulijn, J. A., *Prep. Am. Chem. Soc., Div. Petr. Chem.* **39**, 571 (1994).
20. Ng, K. T., and Hercules, D. M., *J. Phys. Chem.* **80**, 2094 (1976).
21. Breysse, M., Cattenot, M., Decamp, T., Frety, R., Gachet, C., Lacroix, M., Leclerq, C., De Mourgues, L., Portefaix, J. L., Vrinat, M., Horeau, M., Grimblot, J., Kasztelan, S., Bonnelle, J. P., Housni, S., Bachelier, J., and Duchet, J. C., *Catal. Today* **4**, 39 (1988).
22. Reinhoudt, H. R., Van der Meer, Y., Van der Kraan, A. M., Van Langeveld, A. D., and Moulijn, J. A., *Fuel Proc. Technol.*, submitted.
23. Mangnus, P. J., Riezebos, A., Van Langeveld, A. D., and Moulijn, J. A., *J. Catal.* **151**, 178 (1995).
24. Reinhoudt, H. R., Mariscal, R., Van Langeveld, A. D., De Beer, V. H. J., Van Veen, J. A. R., Sie, S. T., and Moulijn, J. A., *Prepr. 213 ACS National Meeting, Div. Petr. Chem., San Francisco, CA, April 13–17, 1997.*
25. Eijsbouts, S., Heinerman, J. J. L., and Elzerman, H. J. W., *Appl. Catal. A General* **105**, 53 (1993).
26. Zandbergen, H. W., and Trœholt, C., Small particles, catalysis, photography, magnetic recording, *in* "Handbook of Microscopy, Applications in Materials Science, Solid State Physics and Chemistry" (S. Amelinckx, D. van Dyck, J. van Landuyt, and G. van Tendeloo, Eds.), VCH, Weinheim, 1997.
27. Scheffer, B., Heijinga, J. J., and Moulijn, J. A., *J. Phys. Chem.* **91**, 4752 (1987).